REGULARIZATION FOR INVERTING THE RADON TRANSFORM WITH WEDGE CONSIDERATION

By

I. Aganj, A. Bartesaghi, M. Borgnia

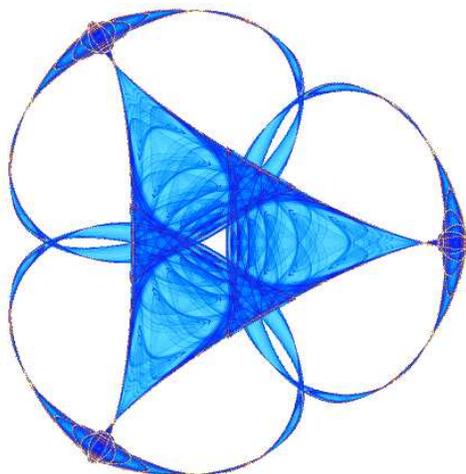**H.Y. Liao, G. Sapiro**

and

S. Subramaniam

INSTITUTE FOR MATHEMATICS AND ITS APPLICATIONS

REGULARIZATION FOR INVERTING THE RADON TRANSFORM WITH WEDGE CONSIDERATION

I. Aganj[1], A. Bartesaghi[2], M. Borgnia[2],

H.Y. Liao [3], G. Sapiro[1] and S. Subramaniam[2]

[1]Dept. of Electrical Engineering
[3]Inst. for Mathematics and Its Appl.
University of Minnesota
Minneapolis, MN 55455, USA

[2]Center for Cancer Research
National Institutes of Health
50 South Drive, MSC 8008
Bethesda, MD 20892-8008

ABSTRACT

In limited angle tomography, with applications such as electron microscopy, medical imaging, and industrial testing, the object of interest is scanned over a limited angular range, which is less than the full $180°$ mathematically required for density reconstruction. The use of standard full-range reconstruction algorithms produces results with notorious "butterfly" or "wedge" artifacts. In this work we propose a reconstruction technique with a regularization term that takes into account the orientation of the missing angular range, also denoted as *missing wedge*. We show that a regularization that penalizes non-uniformly in the orientation space produces reconstructions with less artifacts, thereby improving the recovery of the "invisible" edges due to the missing wedge. We present the underlying framework and results for a challenging phantom and real cryo-electron microscopy data.

Keywords: *Limited angle tomography, missing wedge, non linear regularization, directional smoothing*

1. INTRODUCTION

Tomography refers to the recovery of the density distribution of an object from its (noisy) projections, and it is mathematically related to the Radon transform. It is well known that the problem of density reconstruction from its real projections is ill-posed, and various algorithms have been proposed for addressing this, e.g., [1, 2]. These algorithms typically work reasonably well when the data are collected over a complete angular range of 180 degrees. Roughly stated, the basic reconstruction techniques apply explicitly or implicitly some sort of regularization either in the frequency domain or in the image domain. In many cases however (e.g. due to mechanical constraints in electron tomography) only a limited angular range of projections is available, generating the so called *missing wedge* of information. To see the effect of the missing wedge, the top-right image of Fig. 1 shows the result of reconstruction by standard Filtered Back-Projection (FBP) of
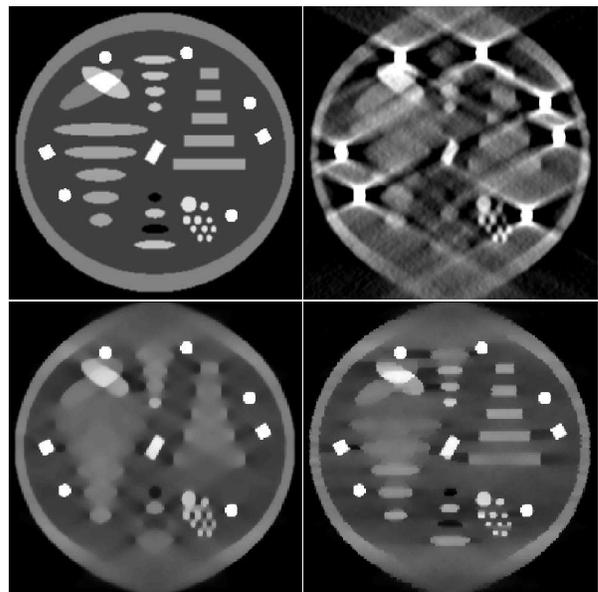
Fig. 1. *A phantom of the type used in [3] (top-left); its FBP reconstruction (linear interpolation, Hanning filter, and cutoff 0.8) (top-right); reconstruction using standard non-linear regularization (bottom-left); and our proposed directional smoothing (bottom-right). The mean squared errors are respectively 0.0131, 0.0016, and 0.0012. All the images are 240 × 240 and displayed in the range [0, 0.4]. The missing wedge is $60°$.*

a phantom, shown on its left, that is of the type introduced in [3]. The FBP is a standard full-range reconstruction algorithm that, in its simplest version, sets the Fourier coefficients in the missing wedge to zero, which in this example is $60°$ (as typical in electron tomography). Here, the reconstruction is displayed in the density range [0, 0.4]. (Most of the low density features in the phantom are valued in the range 0.2-0.4, while the densest is valued at 2.05; see [3] for details.)

In the presence of a missing wedge, standard full-range reconstruction algorithms fail to produce satisfactory results, and therefore more specific approaches such as Fourier methods, sinogram methods, regularization methods, and wavelet

techniques, have been proposed (see, e.g., references cited in [3] and more recently [4, 5]). However, to the best of our knowledge, these methods derive directly from their standard full-range versions, without special consideration of the specific geometry of the missing wedge. Therefore, these techniques are still vulnerable to wedge artifacts, unless a reference image is used which is nevertheless not always available.

Based on the well-known central slice theorem (see, e.g., [2]), it is easy to see that edges parallel to the available projection rays can be recovered, but this is not the case for those that are parallel to the missing rays, which become invisible in the reconstructions. Therefore, a method that applies isotropic (linear or non-linear) smoothing, which does not make distinction between the visible and the invisible edges, would have limited usefulness. In this work we propose a smoothing term that penalizes invisible edges the least possible. In our regularization formulation, we have a weighted sum of an isotropic smoothing and a directional smoothing along the average direction of the missing rays. The first has the effect of global regularization, whereas the latter minimally penalizes the invisible edges. We found that wedge artifacts are thus reduced, thereby improving the quality of the recovered structures. The bottom row of Fig. 1 shows the results of isotropic smoothing and our proposed smoothing, both displayed in the density range [0, 0.4]. Compared with the isotropic smoothing and with the regularization method in [3] (which uses non-convex optimization and relies on a good starting image), our method better recovers the structure, while the problem is still convex.

In Section 2 we present and justify our approach, and give the experimental settings and results in Section 3, both for a phantom of the type used in [3] and real cryo-tomography data. In the last section we provide discussions and conclusions.

2. ANISOTROPIC REGULARIZATION

Total Variation (TV) regularization [6] has been shown to be very useful in several image processing tasks. Applications to image reconstruction in tomography have also been reported [4]. Here we advocate the use of a smoothing in the average direction of the missing rays, in addition to the TV smoothing, which is isotropic.

In a standard image denoising problem, where the noise is usually isotropic and hence edges of different orientations are equally affected, TV regularization (to be explained shortly) has been shown to be capable of recovering sharp edges. However, in tomography, it is easy to verify (using the central slice theorem; see also [7]) that the micrographs provide information regarding only the edges that are parallel to the available projection rays. This means that when there is a missing wedge, edges that are parallel to the missing rays cannot, in principle, be recovered. The preceding observation is clearly reflected in results using standard full-range reconstruction al-

gorithms and even most current methods (see, e.g., the horizontal edges of the top-right image of Fig. 1, which is a reconstruction by FBP from rays oriented from 30° to 149°).

Thus, incorporating a TV-type regularization in limited angle tomography should be done carefully. On one hand we would like the visible edges (those that can be recovered) to be sharp. On the other hand, we do not wish to penalize too much the invisible edges, those that were not explicitly captured by the projections due to the missing wedge. We propose to consider a smoothing composed of a low weighted TV combined with a penalty along the average direction of the missing rays, which we show below that it is the optimal direction that minimally penalizes the invisible edges. To simplify the discussions, we consider 2D images; generalization to 3D is straightforward.

We propose as image solution of the inverse projection problem a function $F(x, y)$, defined on a bounded open domain $\Omega \in \mathbb{R}^2$, that is a minimizer of the functional

$$\lambda_1 \int_\Omega \sqrt{\left(\frac{\partial F}{\partial x}\right)^2 + \left(\frac{\partial F}{\partial y}\right)^2} \, dx \, dy + \tag{1}$$

$$\lambda_2 \int_\Omega \left|\frac{\partial F}{\partial x}\right| dx \, dy + \frac{1}{2} \int_\Gamma (\Re F - w)^2 \, dt \, d\phi,$$

where $\Re$ is the Radon transform that depends on the scanning geometry. Γ comprises all the rays along which the data w have been collected. Variable t parameterizes the rays in one view, and ϕ, which is the angle of the rays plus $90°$, ranges between $-\alpha$ and α with $0° < \alpha \leq 90°$. (The angle α used in the reconstructions of Fig. 1 is $60°$, representing the typical size of the missing wedge.) Thus, the central missing ray (which is also the average direction of the missing rays) is oriented horizontally, i.e. the x direction. The parameters λ_1 and λ_2 are the weights of, respectively, the TV smoothing and the newly added directional smoothing. The last term is the so called *fidelity*. The TV term is isotropic along the x and y directions, while the directional smoothing penalizes only in the x direction. Assuming uniform probability for the edge directions in the density data, it is easy to see that the penalty of the invisible edges along a direction $\widehat{\omega}$, defined by $\int_\alpha^{180°-\alpha} |\nabla F \cdot \widehat{\omega}| \, d\theta$, where $\widehat{\omega} = (\cos\omega, \sin\omega)$ and $\nabla F = (\cos\theta, \sin\theta)$ (so that $F(x, y)$ has an edge of θ degrees and unit jump at (x, y)), is minimized for $\omega = 0°$; i.e., the x direction. This is thereby the optimal regularization direction, the one in the middle of the wedge[1]. With a reasonable λ_2, we do not expect that this directional smoothing penalizes too much the visible edges, since the projection data already contain some information about them. It is also intuitive to see that a larger λ_2 (relative to λ_1) is needed as either the miss-

---

[1] This can also be derived from simple symmetry considerations. Due to linearity, it is also easy to show that there is no gain in penalizing for multiple directions covered by the wedge. If the edge directions in the data are not equally distributed, this optimal direction can be derived to take this non-uniform probability into consideration.

ing wedge gets larger or there are more horizontally elongated shapes in the image.

We adopt a finite difference framework to solve (1) for $F(x, y)$, using a discretization of the Radon transform. Note that our functional is convex, which is easier to optimize than a non-convex one. We use the gradient descent method with explicit scheme to find the minimizer of (1). We also tested semi-implicit schemes based on the works in [8, 9], but did not find significant improvements over the explicit scheme in terms of speed.

3. EXPERIMENTS

3.1. Phantom data

In order to compare our approach with the work in [3], we created a phantom (see Fig. 1) that is almost identical to that in [3], which contains numerous horizontally elongated primitives of various shapes. The central missing ray is also horizontal (this of course does not limit the generality of the approach; it is just an example for a given direction of the wedge and data). The reason for choosing such shapes is because the recovery of horizontal elongation is more challenging than with any other elongation direction for the given missing wedge range. Most of the low density primitives are valued in the range 0.2-0.4, while the densest is valued 2.05. A detailed quantitative description of the phantom can be found in [3].

The remaining three images in Fig. 1 are reconstructions by three different methods (FBP, TV regularization, and our proposed method), and they are displayed in the density range [0,0.4]. All the images are 240×240, and the simulated noisy projection data consist of 120 views that correspond to 120 consecutive degrees (i.e., the missing wedge is $60°$). The noise was assumed to be Gaussian with 0.5 standard deviation, which resembles the noise level in [3], corresponding to the case when the Poisson count is $2 \cdot 10^5$. Next to the phantom is the reconstruction by a FBP with Hanning filter and cutoff 0.8. Here, the wedge artifact is very prominent especially for the high density objects, and most of the low density primitives are distorted or unrecognizable. The bottom left image is a reconstruction by TV regularization (by setting $\lambda_2 = 0$ in (1)), which is an isotropic smoothing. The wedge artifacts are much reduced, but not for the low density primitives, especially the longer rectangles that are discontinuous and the ellipses that become fatter. Finally, a reconstruction by our method shown at the bottom-right exhibits a significantly better recovery of such primitives. The parameters λ_1 and λ_2 in each case were tuned such that they produce visually minimal distortion and artifacts. They are $(\lambda_1, \lambda_2) = (10, 0)$ and $(\lambda_1, \lambda_2) = (1, 10)$, respectively for the isotropic regularization and our regularization. In the gradient descent method, $2 \cdot 10^4$ iterative steps were needed in each case; and the time step was $5 \cdot 10^{-5}$. We also found that our reconstruction is
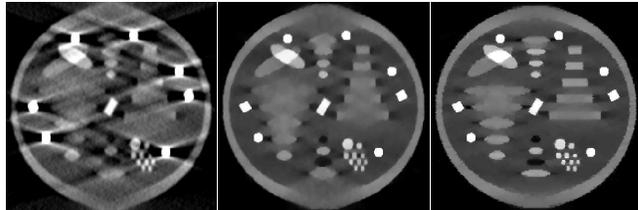
Fig. 2. *Reconstruction of the phantom of Fig. 1 with $40°$ missing wedge, using FBP (left, linear interpolation, Hanning filter, and cut-off 0.8), standard non-linear regularization (center); and our proposed directional smoothing (right). The mean squared errors are respectively 0.008, 0.0011, and 0.0006. All the images are 240 × 240 and displayed in the range [0, 0.4].*

better than that in [3] in terms of the recovery of the primitives. Figure 2 shows the results of a similar experiment but with a missing wedge of $40°$.

3.2. Cryo-Electron Microscopy Data

We show results of the proposed algorithm applied to Cryo-Electron Microscopy (Cryo-EM) data obtained from bacteria cells embedded in vitreous ice. A tilt series was collected at liquid nitrogen temperature using a Polara field emission gun electron microscope (FEI Company, OR) equipped with a 2k x 2k CCD, and operated at 300 kV. 40 equally spaced projections were collected in the +/-50 degree range with pixel size of .56 nm. Images were properly aligned and normalized to a common reference frame before attempting reconstruction. Cryo-EM data is collected under extremely low electron doses to avoid sample damage from beam radiation in an attempt to get close to native acquisition conditions [10], as a result, projection images have very poor signal-to-noise ratios presenting a challenging example of limited angle tomography reconstruction.

Fig. 3 shows, from left to right, reconstructions together with their sinograms using ART, SIRT, and our method, respectively, of one slice through the bacteria. The Algebraic Reconstruction Techniques (ART; see [1]) and the Simultaneous Iterative Reconstruction Techniques (SIRT; see, e.g., [2]) are two popular reconstruction algorithms, as alternatives to the FBP. We found that, because of the noise in the data, we could not run too many iterations in any of the three algorithms; otherwise, the reconstruction would start to fit the noise and lose the signal.

Therefore, noting that only for very high smoothing parameters were we able to run more iterations in our method, we used a decreasing sequence of parameters during the iterations. We started with $(\lambda_1, \lambda_2) = (750, 300)$ and ran for 300 iterations, followed by $(75, 30)$ for 300 iterations, then $(7.5, 3)$ for 20 iterations, and finally $(0, 0)$ for another 20 iterations. Here, as opposed to the previous case where the phantom contains numerous highly elongated structures, the
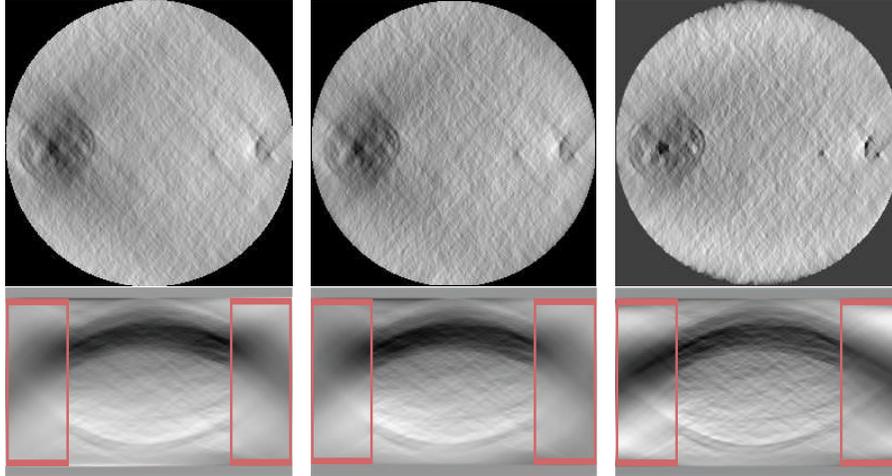
Fig. 3. *Reconstructions (256 × 256) and their sinograms using ART (left), SIRT (center), and our directional smoothing method (right). Each of the two boxes in each sinogram encloses half of the missing wedge. Note that, unlike the first two sinograms, which diffuse into the missing wedge zone, the last sinogram extends much nicely into it.*

shapes are mostly rounded and small, therefore we need a smaller λ_2 relative to λ_1. In fact, in this case, the result is not very sensitive to the parameters. As can be seen, compared with standard ART (pixel-basis, relaxation parameter 0.1 and 20 cycles through the data) and SIRT (pixel basis, relaxation parameter $5 \cdot 10^{-5}$ and 20 iterations), our method with decreasing parameters produces a reconstruction with higher contrast and more revealing features in the image. The sinogram, displayed from $-90°$ to $90°$, of our directional smoothing method also shows better continuation.

4. CONCLUSIONS AND DISCUSSIONS

We have introduced a new anisotropic regularization method for limited angle tomography. We argue that, due to the missing wedge, more smoothing should be applied in the average direction of the missing rays. We have justified and also demonstrated experimentally this fact on a challenging phantom. Reduced wedge artifacts and sharper recovered shapes were achieved, using our proposed anisotropic smoothing, as compared to the total variation smoothing that is isotropic. Examples with real Cryo-EM data were presented as well.

Acknowledgment

5. REFERENCES

[1] G.T. Herman, *Image Reconstruction from Projections: The Fundamentals of Computerized Tomography*, Academic Press, New York, 1980.

[2] F. Natterer and F. Wuebbeling, *Mathematical Methods in Image Reconstructions*, SIAM, Philadelphia, 2001.

[3] A.H. Delaney and Y. Bresler, "Globally convergent edge-preserving regularized reconstruction: an application to limited-angle tomography," *IEEE. Trans. Imag. Proc.*, vol. 7, pp. 204–221, 1998.

[4] M. Persson, Bone T., and H. Elmqvist, "Total variation norm for three-dimensional iterative reconstruction in limited view angle tomography," *Phys. Med. Biol.*, vol. 46, pp. 853–866, 2001.

[5] M. Rantala, S. Vänskä, Järvenpää S., Kalke M., Lassas M., Moberg J., and S. Siltanen, "Wavelet-based reconstruction for limited angle X-ray tomoraphy," *IEEE Trans. Med. Imag.*, vol. 25, pp. 210–217, 2006.

[6] L. Rudin, S. Osher, and C. Fatemi, "Nonlinear total variation based noise removal algorithms," *Physica D*, vol. 60, pp. 259–268, 1992.

[7] E.T. Quinto, "Singularities of the X-ray transform and limited data tomography," *SIAM J. Math Anal.*, vol. 5, pp. 1215–1225, 1993.

[8] A. Chambolle, "An algorithm for total variation minimization and applications," *J. Math. Imaging Vis.*, vol. 20, pp. 89–97, 2004.

[9] T.F. Chan, G.H. Golub, and P. Mulet, "A nonlinear primal-dual method for total variation-based image restoration," *SIAM J Sci. Comput.*, vol. 20, pp. 1964–1977, 1999.

[10] S. Subramaniam and J. L. S. Milne, "Three-dimensional electron microscopy at molecular resolution," *Ann. Rev. Biophys. and Biomol. Struct.*, vol. 33, June 2004.